

## Redundant and unique roles of coronin proteins in *Dictyostelium*

Maria C. Shina · Annette Müller-Taubenberger · Can Ünal · Michael Schleicher ·  
Michael Steinert · Ludwig Eichinger · Rolf Müller · Rosemarie Blau-Wasser ·  
Gernot Glöckner · Angelika A. Noegel

Received: 3 February 2010/Revised: 23 May 2010/Accepted: 5 July 2010/Published online: 18 July 2010  
© Springer Basel AG 2010

**Abstract** *Dictyostelium discoideum* harbors a short (CRN12) and a long coronin (CRN7) composed of one and two beta-propellers, respectively. They are primarily present in the cell cortex and cells lacking CRN12 (*corA*<sup>-</sup>) or CRN7 (*corB*<sup>-</sup>) have defects in actin driven processes. We compared the characteristics of a mutant cell line (*corA*<sup>-</sup>/*corB*<sup>-</sup>) lacking CRN12 and CRN7 with the single mutants focusing on cytokinesis, phagocytosis, chemotaxis

and development. Cytokinesis, uptake of small particles, and developmental defects were not enhanced in the *corA*<sup>-</sup>/*corB*<sup>-</sup> strain as compared to the single mutants, whereas motility and phagocytosis of yeast particles were more severely impaired. It appears that although both proteins affect the same processes they do not act in a redundant manner. Rather, they often act antagonistically, which is in accordance with their proposed roles in the actin cytoskeleton where CRN12 acts in actin disassembly whereas CRN7 stabilizes actin filaments and protects them from disassembly.

M. C. Shina · L. Eichinger · R. Müller · R. Blau-Wasser ·  
A. A. Noegel  
Institute for Biochemistry I, Center for Molecular Medicine  
Cologne (CMMC) and Cologne Excellence Cluster on Cellular  
Stress Responses in Aging-Associated Diseases (CECAD),  
Medical Faculty, University of Cologne,  
50931 Cologne, Germany

A. Müller-Taubenberger · M. Schleicher  
Institute for Cell Biology and Center for Integrated Protein  
Science (CIPSM), Ludwig Maximilians University Munich,  
80336 Munich, Germany

C. Ünal · M. Steinert  
Institute for Microbiology, Technical University Braunschweig,  
38106 Brunswick, Germany

G. Glöckner  
Leibniz Institute for Freshwater Ecology and Inland Fisheries,  
Müggelseedamm 301, 12587 Berlin, Germany

A. A. Noegel (✉)  
Institute for Biochemistry I, Medical Faculty,  
University of Cologne, Joseph-Stelzmann-Str. 52,  
50931 Cologne, Germany  
e-mail: noegel@uni-koeln.de

### Present Address:

C. Ünal  
Medical Microbiology, Department of Laboratory Medicine,  
Malmö, University Hospital, Lund University,  
205 02 Malmö, Sweden

**Keywords** Actin cytoskeleton · Coronin · Cell motility ·  
Phagocytosis · Development

### Introduction

The coronin gene family has members in vertebrates, nonvertebrate metazoa, fungi and protozoa, but no representatives in plants or distant protists. Coronins are characterized by WD (tryptophan-aspartic acid) repeats that form a seven-bladed  $\beta$ -propeller as in the  $\beta$ -subunit of G proteins [1] followed by C-terminal extensions and a coiled coil domain which mediates oligomerization [2].

They have been associated with actin dynamics like the control of F-actin assembly and the regulation of the Arp2/3 complex [3, 4]. Moreover, actin binding can be considered the landmark feature of coronins and actin binding sites have been mapped to various parts of the coronin paralogues [5–7]. The first coronin (now designated CRN12) was isolated from *Dictyostelium discoideum* as a major co-purifying protein in a preparation of contracted actomyosin and the analysis of *corA*<sup>-</sup> cells revealed roles in cell migration, phagocytosis and cell division [8–10]. Actin association and

its sequence relation to the  $\beta$ -subunit of G proteins implicated a role for coronin as an important regulator of the actin cytoskeleton. Further studies showed that coronins may also have actin-independent roles. In *Saccharomyces cerevisiae* and *Leishmania donovani*, coronin associates with microtubules and regulates microtubule remodeling during *Leishmania* cytokinesis [11–13], mammalian coronin 1 (synonyms: Coronin 1a, CRN4) has a role in activating  $\text{Ca}^{2+}$  dependent signaling processes [14].

Most eukaryotes harbor in addition to small coronins with one WD-repeat domain a coronin gene encoding two WD-repeat domains designated POD or CRN7 that form two separate  $\beta$ -propellers [15]. In *D. discoideum* and *Drosophila melanogaster* they are cytoskeletal components and bind directly to F-actin [16, 17], whereas mammalian CRN7 associates with Golgi membranes and affects membrane trafficking [18, 19]. Mutations in the *D. melanogaster* and *Caenorhabditis elegans* CRN7 homologues (Pod proteins) lead to polarity defects, loss of *D. discoideum* CRN7 causes alterations in chemotaxis and phagocytosis. Furthermore, in *D. discoideum* CRN7 deficiency affects the infection process by *Legionella pneumophila*, the causative agent of Legionnaire's disease, and allows a more efficient internalization of bacteria [16]. CRN12 also has a role during infection as its absence resulted in enhanced intracellular replication of *Mycobacterium marinum*, a pathogen causing tuberculosis-like disease in fish and amphibians, and *L. pneumophila* relative to the wild-type strain [20, 21].

Here, we compare the in vivo functions of the two *Dictyostelium* coronins CRN12 encoded by the *corA* gene and CRN7 encoded by *corB* by analyzing mutants lacking either one or both coronin proteins with a focus on processes that require the actin cytoskeleton. Previous work had shown that CRN12 and CRN7 interacted directly with F-actin in vitro. CRN12 co-sedimented with actin filaments, CRN7 exhibited similar properties and protected F-actin from depolymerization [8, 16], whereas results from live cell imaging led to the proposal that CRN12 plays a role in actin disassembly [22]. Direct biochemical data are however lacking.

In this report, we follow the new nomenclature for the coronins, which was recently proposed by Morgan and Fernandez and is based on phylogenetic considerations [23].

## Materials and methods

### Development, growth, and transformation of *Dictyostelium*

Strains were cultivated in shaking suspension or in submerged culture at 21°C in axenic medium [24].

Development was initiated by plating  $5 \times 10^7$  cells on a phosphate agar plate (10 cm in diameter) and followed over 24 h. Every 30 min pictures were taken. For analysis of stream formation under submerged conditions on a plastic surface,  $2 \times 10^5$  cells/cm<sup>2</sup> were starved under Sorensen phosphate buffer (2 mM  $\text{Na}_2\text{HPO}_4$ , 14.6 mM  $\text{KH}_2\text{PO}_4$ , pH 6.0) and monitored for aggregation. The mutant cell lines were maintained in the presence of 5  $\mu\text{g}/\text{ml}$  Blasticidin (MP Biomedicals Inc.) or 10–20  $\mu\text{g}/\text{ml}$  of G418 (Roche). To generate mutant cells lacking *corA* and *corB*, the *corB* gene was inactivated in *corA*<sup>-</sup> mutants (HG1569) where the *corA* gene had been inactivated using a gene replacement vector which carried a G418 resistance cassette [9]. For *corB* inactivation the replacement vector described for the inactivation of *corB* in Ax2 was used [16]. Transformants were screened by PCR and confirmed by Southern and Northern-blot analysis. Cell lines used were Ax2 (wild-type), *corA*<sup>-</sup>, *corB*<sup>-</sup> and *corA*<sup>-</sup>/*corB*<sup>-</sup>. A detailed characterization of the *corB* mutant has been reported previously [16]. The analysis of *corA*<sup>-</sup> and *corA*<sup>-</sup>/*B*<sup>-</sup> cells has been carried out in parallel. Therefore, data for Ax2 wild-type and *corB*<sup>-</sup> are identical to the ones previously reported in some instances. This is indicated in the figure legends.

### Phagocytosis assays

Quantitative phagocytosis of TRITC-labeled heat-killed yeast cells was performed as described [10]. The phagocytosis was also assayed on a substratum where the cells were allowed to settle on coverslips and yeast cells were added. After 15 min the cells were fixed in methanol, stained for actin [16] and embedded. Between 200 and 400 cells were analyzed for uptake of yeast particles. For quantitative analysis of phagocytosis of bacteria pHrodo *E. coli* conjugates (Invitrogen) were used. Because the fluorescence of the pHrodo dye dramatically increases as the pH decreases from neutral to acidic, it is an ideal tool to study phagocytosis and its regulation by drugs or environmental factors. The lack of dye fluorescence outside the cell eliminates the need for washing steps and quencher dyes ([www.invitrogen.com](http://www.invitrogen.com)). *Dictyostelium* cells were harvested and adjusted to a density of  $2 \times 10^6$  cells/ml. 100  $\mu\text{l}$  ( $2 \times 10^5$  cells) aliquots each were pipetted into the wells of a 96-well plate (labsystems CLINIPLATE) and incubated for at least 1 h. During this time, the pHrodo Bio particles were dissolved in a buffer containing 20 mM HEPES, 2 mM  $\text{MgCl}_2$  and 10 mM NaCl, adjusting the pH to 7.4 with NaOH and sonicated for 5 min in a water bath sonifier. One vial of these conjugates is sufficient for 20 wells. The culture medium from the *D. discoideum* cells was removed and quickly displaced by 100  $\mu\text{l}$  of the prepared pHrodo *E. coli* BioParticles (invitrogen). The

**Table 1** The Coronin family in the *Dictyostelia*

Coronin subfamily	Gene	Species	Gene ID	Length (amino acids)	% Identity with <i>D. d.</i> Protein
CRN12	<i>corA</i>	<i>D. discoideum</i>	DDB_G0267382	445	
	<i>corA</i>	<i>P. pallidum</i>	PPL_02337	447	78.33
	<i>corA</i>	<i>D. fasciculatum</i>	DFA_04446	447	83.33
CRN7	<i>corB</i>	<i>D. discoideum</i>	DDB_G0269388	963	
	<i>corB</i>	<i>P. pallidum</i>	PPL_06027	920	61.81
	<i>corB</i>	<i>D. fasciculatum</i>	DFA_06579	984	73.68

The genomes of *P. pallidum* and *D. fasciculatum* were searched at <http://sacgb.fli-leibniz.de/cgi/index.pl> using the sequences for *D. discoideum* CRN12 and CRN7 (available at <http://dictybase.org/index.html>)

microplate was transferred into the Labscan Fluoroscan Ascent FL and the phagocytosis experiment started measuring fluorescence at ~550 nm excitation and ~660 nm emission. After subtraction of the control values the relative fluorescence was determined.

#### Miscellaneous methods

Analysis of cell shape and cell migration during chemotaxis was done as described [16], *Legionella* infection is described in Peracino et al. [25]. MAbs 176-3-6 and K67-146-1 specific for CRN12 and CRN7 have been used in this study [8, 16], act-1 recognized actin [26]. For DMSO treatment cells on coverslips were kept in culture medium supplemented with 5% DMSO for the indicated time at 22°C, fixed with methanol and immunostained for actin with mAb act-1. Analysis was with a Leica TCS SP5 confocal microscope (Leica, Wetzlar, Germany). For analysis of mitotic microtubule structures, cells were treated with nocodazole (10 µM) for 3 h [27]. Cells were fixed with cold methanol, microtubules were stained with the  $\alpha$ -tubulin antibody YL1/2 [28], nuclei were stained with DAPI. The number of cells in prophase to metaphase with no microtubules and cells with a normal microtubule cytoskeleton were determined for each strain. The experiment was carried out twice. At least 1,000 cells per strain were analyzed.

## Results

### Comparison of CRN12 and CRN7

*D. discoideum* harbors a small (monomeric) and a long (dimeric) coronin of 445 (CRN12) and 963 (CRN7) amino acids encoded by the *corA* and *corB* gene, respectively. Overall, the proteins share 18.1% identity with each other when directly compared. When we compare the individual WD-repeat domains we find that the C-terminal WD-repeat domain of CRN7 is more closely related to CRN12 (30.7%

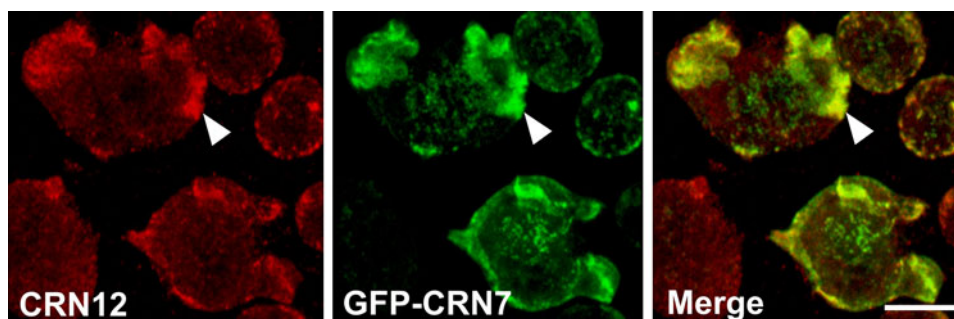
identity) than the N-terminal WD-repeat domain (26.2% identity). CRN12 and CRN7 are also present in other social amoebae species where they are highly conserved. We identified a small and long coronin each in the genomes of *Polysphondylium pallidum* and *Dictyostelium fasciculatum*. *P. pallidum* and *D. fasciculatum* belong to family 2 and family 1 of the *Dictyostelia*, *D. discoideum* is a member of group 4 [29]. CRN12 from *P. pallidum* and *D. fasciculatum* were 78.33% and 83.33% identical to *D. discoideum* CRN12, the CRN7 proteins from *P. pallidum* and *D. fasciculatum* were 61.81 and 73.68% identical to *D. discoideum* CRN7 (Table 1). All CRN12 proteins have the coronin signature RxxKxR near the amino terminus (position 6–13 of *D. discoideum* CRN12), in *D. discoideum* CRN7 the N-terminal signature is changed to KxxKxR, whereas the signature in front of the second WD-repeat domain (residues 489–494) is identical to the CRN12 signature [30].

### Generation of *corA*<sup>-</sup>/*corB*<sup>-</sup> mutants

CRN7 and CRN12 associate with the actin cytoskeleton and have a similar subcellular localization. When we stained GFP-CRN7 expressing cells with a monoclonal antibody specific for CRN12 we observed CRN12 in the cell cortex where it accumulated at phago- and pinocytic cups as described [10]. It co-localized with CRN7 in particular at macropinosomes and at the cell periphery. The staining did however not completely overlap as CRN12 showed a more diffuse cytoplasmic distribution whereas CRN7 was also present in dot-like structures whose identity is not known (Fig. 1).

The generation and characterization of *corA*<sup>-</sup> and *corB*<sup>-</sup> mutants has been described previously [9, 16]. Here we compared their in vivo functions directly and included *corA*<sup>-</sup>/*corB*<sup>-</sup> mutant cells that were generated by introducing a CRN7 gene replacement vector into *corA*<sup>-</sup> cells. Southern-blot analysis showed the substitution of the endogenous *corB* gene by the replacement vector (Fig. 2a). In Western-blot analysis of total protein extracts with mAb 176-3-6 and K67-146-1 [9, 16] no CRN12 and CRN7

**Fig. 1** GFP-CRN7 and endogenous CRN12 co-localize to a large extent. GFP-CRN7 expressing cells were fixed and co-stained for CRN12 with mAb 176-3-6. The *arrowhead* points to areas of colocalization. *Bar* 8  $\mu$ M



protein was detected in the double knockout (Fig. 2b). In our subsequent analysis we focused on growth, cytokinesis, chemotaxis, development and phagocytosis behavior.

Growth in axenic medium was altered for all coronin mutants. They grew more slowly and did not reach the same final densities at the stationary phase as Ax2. *corA*<sup>-</sup> cells showed the highest impairment followed by *corA*<sup>-</sup>/*corB*<sup>-</sup> and *corB*<sup>-</sup> cells. (Fig. 2c).

For *corA*<sup>-</sup> mutants an increased cell size associated with multinuclearity has been reported, *corB*<sup>-</sup> cells are nearly indistinguishable from the parental Ax2 strain with regard to size and nuclei number [9, 16]. The *corA*<sup>-</sup>/*corB*<sup>-</sup> double mutant was similar in size to Ax2 and showed a decrease in the number of large multinucleated cells as compared to *corA*<sup>-</sup>. Whereas almost 50% of all *corA*<sup>-</sup> cells had three and more nuclei, this number dropped to 20% for the *corA*<sup>-</sup>/*corB*<sup>-</sup> cells. The majority of Ax2 and *corB*<sup>-</sup> cells had one and two nuclei (Fig. 2d).

The cell cortex is organized during mitosis in conjunction with the microtubule system and defects in either one might be reflected in changes during mitosis. A hint for this proposal was the finding that the position of the asters coincides with areas of the cell cortex where CRN12 accumulates [31]. We next analyzed the frequency of mitotic stages after Nocodazole treatment which alters microtubule dynamics and determined the number of cells in pro- and metaphase. We observed clear differences in all strains. Whereas 18.4% Ax2 cells were in these stages of mitosis, we determined for *corA*<sup>-</sup> only 3.5%, for *corB*<sup>-</sup> 4.7% and for *corA*<sup>-</sup>/*B*<sup>-</sup> 6.5% (Fig. 2e).

*corA*<sup>-</sup>, *corB*<sup>-</sup> and *corA*<sup>-</sup>/*corB*<sup>-</sup> strains show defects in chemotaxis, the F-actin response after cAMP stimulation and development

*D. discoideum* lives as single cell amoeba when food is abundant, upon starvation the amoebae aggregate and undergo a developmental cycle resulting in the formation of a fruiting body [32]. Mutants with defects in the actin cytoskeleton often exhibit changes in development. Such changes are thought to result from altered cell shape and chemotactic motility, which are caused by lack of actin

cytoskeleton associated proteins or by proteins regulating the changes in the cytoskeleton [33, 34]. We carried out chemotaxis experiments and analyzed the accompanying cell shape changes in order to compare the impact of the coronins on migration and cell polarity.

During migration towards an exogenous cAMP source, wild-type cells were well polarized and produced pseudopodia exclusively at the front and very few lateral pseudopods and migrated in a highly directed fashion towards the cAMP source (Table 2, Fig. 3a, b). We have reported previously, that the *corB*<sup>-</sup> cells are slightly smaller and less polarized but chemotaxis was not significantly impaired with regard to speed, however they changed their direction more often initially due to a more random fashion of pseudopod extension [16]. The *corA*<sup>-</sup> mutant did not exhibit a well-directed migration towards cAMP and speed was strongly reduced. Only cells near the cAMP source migrated over a short distance, whereas the majority showed a less oriented migration extending several pseudopods in all directions [9]. The *corA*<sup>-</sup>/*corB*<sup>-</sup> mutant cells migrated even slower than the *corA*<sup>-</sup> cells and in a less persistent way. They were not polarized, however pseudopod extension was not as frequent as in *corA*<sup>-</sup> (Table 2, Fig. 3a, b).

cAMP induces a well-characterized pattern of F-actin accumulation in wild-type cells with F-actin polymerization occurring between 5 and 10 s after a cAMP pulse, a rapid depolymerization and a further lower but longer lasting peak of F-actin accumulation [35]. The first peak is associated with a rounding up of the cells before they extend new pseudopods, which is reflected by the second peak of actin polymerization. The overall pattern was conserved in all strains. We observed a peak of F-actin accumulation at 5 s after cAMP stimulation, however the increase in F-actin content varied. It was lowest in *corA*<sup>-</sup>/*B*<sup>-</sup>, intermediate in *corA*<sup>-</sup>, and *corB*<sup>-</sup> showed the highest F-actin content. After the F-actin disassembly, a second and longer lasting F-actin peak followed in all cell lines (30–40 s) (Fig. 4).

The above results suggest alterations in the regulation of the actin cytoskeleton upon loss of coronin proteins. We tried to obtain independent support for this by following

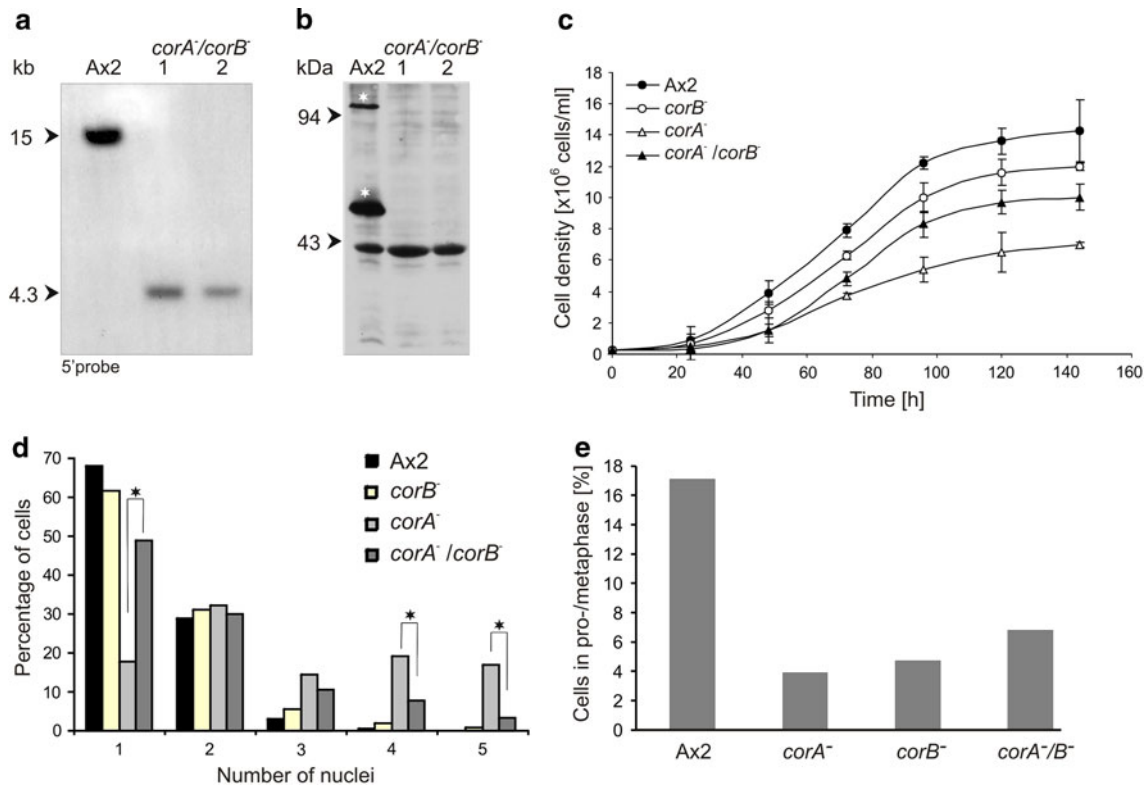


**Fig. 2** Generation of CRN12/CRN7 (*corA*<sup>-</sup>/*corB*<sup>-</sup>) mutants. **a** Southern-blot analysis of SpeI digested genomic DNA of Ax2 and *corA*<sup>-</sup>/*corB*<sup>-</sup> double-mutant cells. Successful insertion of the replacement vector reveals a shift from 15 kb for wild-type to 4.3 kb after digestion with SpeI due to the introduction of an additional SpeI site into the *corB* locus by the bsr cassette after the successful gene replacement event. The gene replacement on chromosome 1 was revealed with a probe located in the gene 5' to *corB* [16]. **b** Western-blot analysis shows the absence of protein in mutant cells. The Western blot was labeled with mAb K67-146-1 (CRN7), mAb 176-3-6 (CRN12), and act 1-7 (actin). Stars indicate CRN7 at 105 kDa and CRN12 at 55 kDa in the wild-type. Actin (at 43 kDa) was used as

loading control. **c** Growth in axenic medium is altered for all coronin mutants.  $2 \times 10^5$  cells/ml were used for inoculation. Over a period of 6 days the cells were counted. All coronin mutant cell lines did not reach the same final densities at the stationary phase as Ax2. The data for Ax2 and *corB*<sup>-</sup> are from Shina et al. [16]. **d** *corA*<sup>-</sup> and *corA*<sup>-</sup>/*corB*<sup>-</sup> cells have a cytokinesis defect. For statistical analysis of multinuclearity of all *coronin* mutants, more than 300 cells per mutant strain were analyzed. Significant changes are indicated by a star. **e** Nocodazole treatment affects mutant cells more severely than Ax2 cells. Cells were treated with nocodazole for 3 h and analyzed for the presence of mitotic cells

**Table 2** Chemotactic behavior in a spatial cAMP gradient

cAMP gradient	Ax2	<i>corB</i> <sup>-</sup>	<i>corA</i> <sup>-</sup>	<i>corA</i> <sup>-</sup> / <i>B</i> <sup>-</sup>
Speed (μm/min)	9.89 ± 2.04	7.58 ± 1.71NS	3.37 ± 0.87***	2.58 ± 0.59***
Persistence (μm/min-deg)	3.82 ± 1.14	2.7 ± 1.27NS	0.84 ± 0.21***	0.59 ± 0.2***
Roundness (%)	54.5 ± 7.15	61.79 ± 6.71NS	72.82 ± 6.03***	64.93 ± 8.31***
Direction change (deg)	13.89 ± 6.29	25.69 ± 10.56**	42.34 ± 12.79***	43.96 ± 9.87***

Images were taken at 40× magnification every 30 s. In all cases cells were recorded over a period of 30 min. Cells were recorded and after tracing of the cells the centroid of the cells was determined by computer-assisted analysis (DIAS). This allows calculations of speed, persistence, roundness (ratio of the long and short axis of the cell), and direction change. Persistence is an estimation of movement in the direction of the path, direction change represents the average change of angle between frames in the direction of movement. The data shown here are derived from five independent experiments, the data for Ax2 and *corB*<sup>-</sup> are from Shina et al. [16]. The data from at least 30 cells were used for statistic evaluation. The statistical significance with respect to wild-type Ax2 cells was calculated using a *t* test; \**p* < 0.05; \*\**p* < 0.01; \*\*\**p* < 0.001; NS not significant at *p* > 0.05

the actin dynamics in cells treated with DMSO. In *D. discoideum* and in mammalian cells incubation with DMSO leads to a reversible disassembly of the cortical actin

cytoskeleton and an accumulation of F-actin as actin rods in the nucleus [36]. We incubated Ax2 and mutant cells in growth medium containing 5% DMSO and followed the

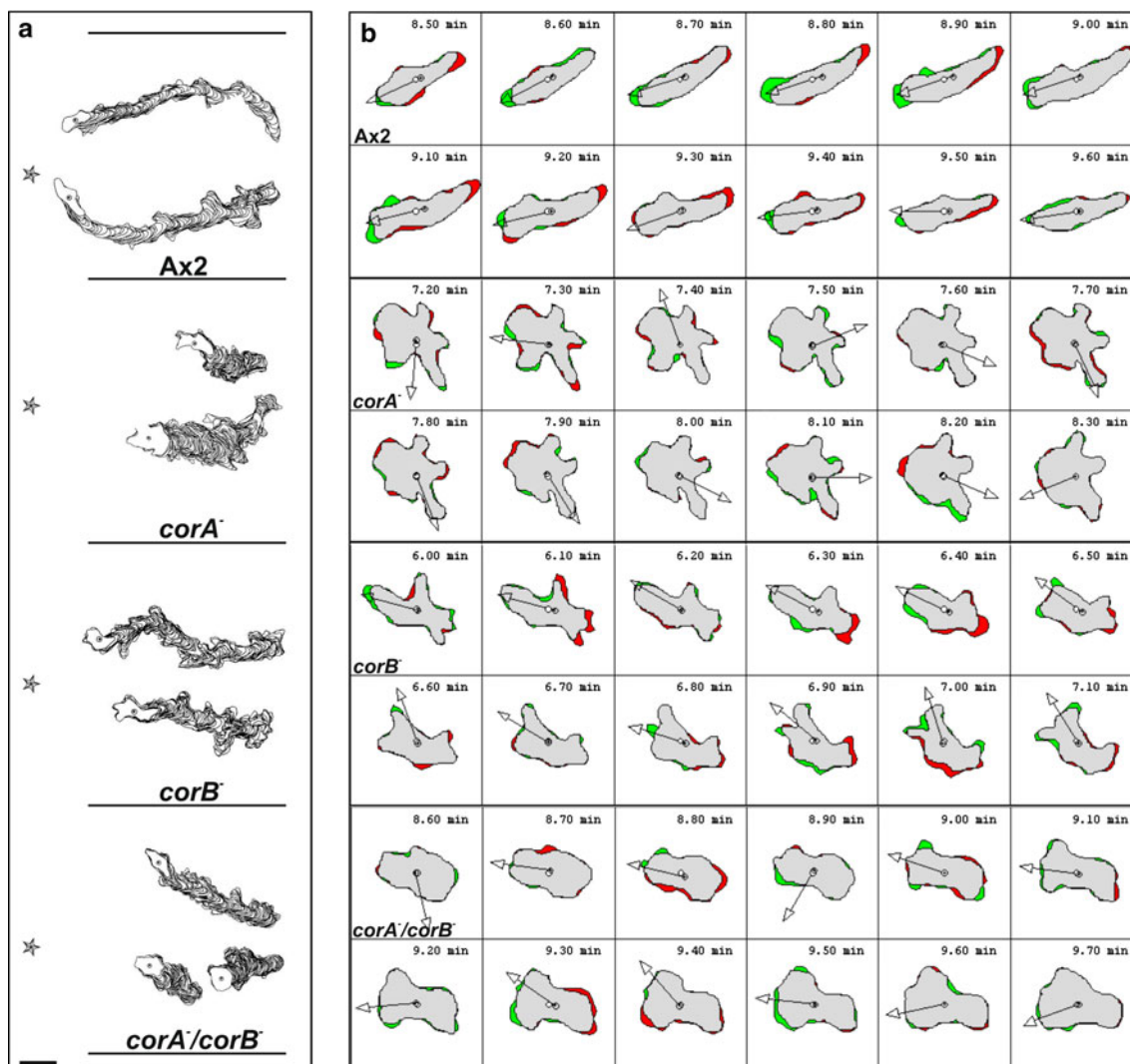


**Fig. 3** Chemotactic movement of coronin mutants is altered. **a** Computer generated cell tracks and stack images of all coronin mutants in comparison to the wild-type Ax2. Aggregation competent cells were deposited on coverslips and after settling down challenged with cAMP. The *star* indicates the location of the pipette filled with cAMP. The cell perimeters were outlined and are shown for two representative cells each. The data for Ax2 and *corB*<sup>-</sup> are from Shina et al.

[16]. *Bar* 8  $\mu$ m. **b** Cell shape changes of aggregation competent mutant and Ax2 cells were analyzed by DIAS software. Images were taken every 10 s. The outlines were traced manually and the changes of direction (*arrows*) calculated using the DIAS image analysis software. The *green areas* indicate new membrane protrusions and the *red areas* retractions

redistribution of actin over a period of 50 min. In Ax2 the characteristic cortical actin staining was completely gone after 30 min and actin rods had formed in the nucleus. In *corA*<sup>-</sup> and *corB*<sup>-</sup> cells cortical actin staining was fragmented and nuclear actin rods were observed after 20 min of incubation, in *corA*<sup>-</sup>/*B*<sup>-</sup> cells similar changes occurred only after 40 min of incubation (Fig. 5).

Development of the strains was analyzed on a plastic surface under submerged conditions and on phosphate agar. Under submerged conditions, cells can aggregate and form streams, but further morphogenesis does not occur. In this experiment the aggregation territories were comparable for all strains, however, stream formation differed.

Wild-type cells formed continuous streams towards the aggregation center. In *corB*<sup>-</sup> cells stream formation occurred in a similar manner but the streams frequently broke up. Streams of *corA*<sup>-</sup> cells appeared more loose and irregular whereas those of the *corA*<sup>-</sup>/*corB*<sup>-</sup> strain were like in wild-type (Fig. 6a).

When we analyzed development on a solid substratum, we observed significant changes for *corA*<sup>-</sup> and *corB*<sup>-</sup> mutants. Ax2 cells develop under starvation conditions within 24 h into fully matured fruiting bodies [32]. Development begins with aggregation after 6 h of starvation followed by the mound and slug stage at 16 h of starvation. *corA*<sup>-</sup> cells have a delay in development by

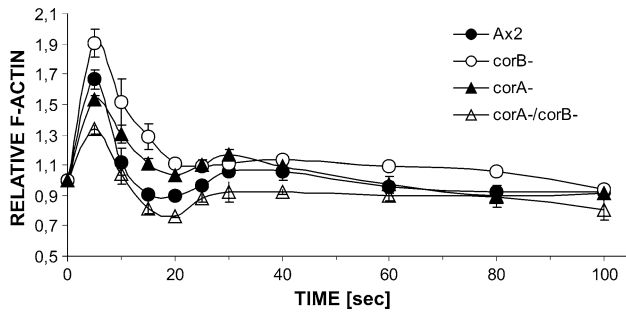


**Fig. 4** F-actin polymerization responses upon cAMP stimulation of aggregation competent cells. Samples were taken at the indicated time points after stimulation with 1  $\mu$ M cAMP. The amount of F-actin was normalized relative to the F-actin level of unstimulated wild-type cells. The relative F-actin content was determined by fluorimetric measurements of TRITC-phalloidin. The data are the average of six independent experiments for each cell line. The data for Ax2 and *corB*<sup>-</sup> are from Shina et al. [16]

approximately 6 h as compared to Ax2 and mature fruiting bodies are formed 30 h after the onset of starvation. *corB*<sup>-</sup> showed accelerated development and had formed aggregates already at the 4 h time point and fruiting bodies after 20 h in comparison to the 24 h needed by Ax2. Development of the *corA*<sup>-</sup>/*corB*<sup>-</sup> strain was comparable to Ax2 (Fig. 6b).

#### The coronins in phagocytosis

Phagocytic pathways in *Dictyostelium* are similar to the ones in mammalian cells [37, 38]. They rely on the actin cytoskeleton and actin-associated proteins play an important role. Both coronins accumulate at the phagocytic cup [10, 12]. Furthermore, for CRN12 a crucial role in phagocytic processes has been well documented. In particular, in experiments with TRITC-labeled yeast CRN12-deficient cells showed a strongly decreased uptake [10]. This

decrease was even stronger in the *corA*<sup>-</sup>/*corB*<sup>-</sup> strain (Fig. 7a). For CRN7-deficient cells we had observed a two-fold higher rate of yeast internalization than for control Ax2 cells [16]. We also investigated whether this phenotype was due to an altered uptake of yeast particles by single cells or to a change in the number of phagocytosing cells by determining the number of intracellular yeast particles after 15 min of phagocytosis. In a representative experiment, 59% of all *corB*<sup>-</sup> cells contained one or two yeast particles, in case of Ax2 34% had ingested one or two yeast cells, for the *corA*<sup>-</sup> mutant we determined 23% and for the double mutant 22% of the cells pointing to different phagocytic properties of the cells. A comparative analysis of uptake of *E. coli*, which are considerably smaller than yeast cells and have different surface properties, showed that all mutant cells exhibited a strong decrease in *E. coli* phagocytosis (Fig. 7b).

CRN7 and CRN12 have distinct roles during infection with *Legionella pneumophila*

*D. discoideum* is frequently used as surrogate host to study infection of cells by pathogenic bacteria. In such studies it was shown that CRN12 has roles during *L. pneumophila* infection as *corA*<sup>-</sup> cells were reported to be more permissive for intracellular growth than wild-type cells [21] and loss of CRN7 allowed a better uptake of the bacteria. In a direct comparison of the *corA*<sup>-</sup>, *corB*<sup>-</sup> and *corA*<sup>-</sup>/*corB*<sup>-</sup>-double knockout strains in standard infection assays using *L. pneumophila* Corby the most remarkable difference noted between the mutants was in the number of intracellular bacteria recovered after gentamicin treatment. While in the case of the *corA*<sup>-</sup> mutant bacterial colony forming units (cfu) after 3 h were comparable to Ax2, the *corB*<sup>-</sup> mutant had internalized about eightfold more

**Fig. 5** Actin dynamics differ in wild-type and mutant strains. Wild-type and mutant cells were incubated in 5% DMSO for the indicated times (min) and immunostained with mAb act1 recognizing actin. DMSO induces a disruption of the actin network. Nuclei were stained with DAPI. Size bars 5  $\mu$ m

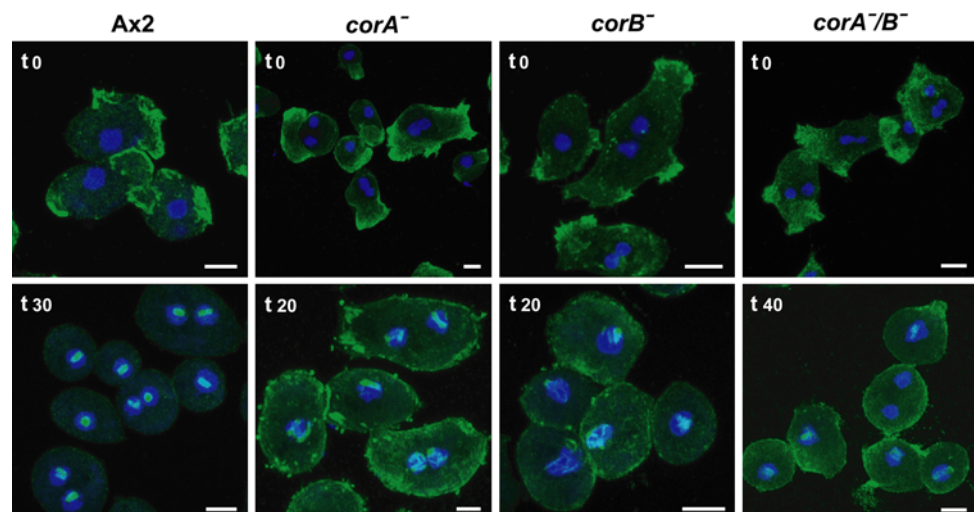
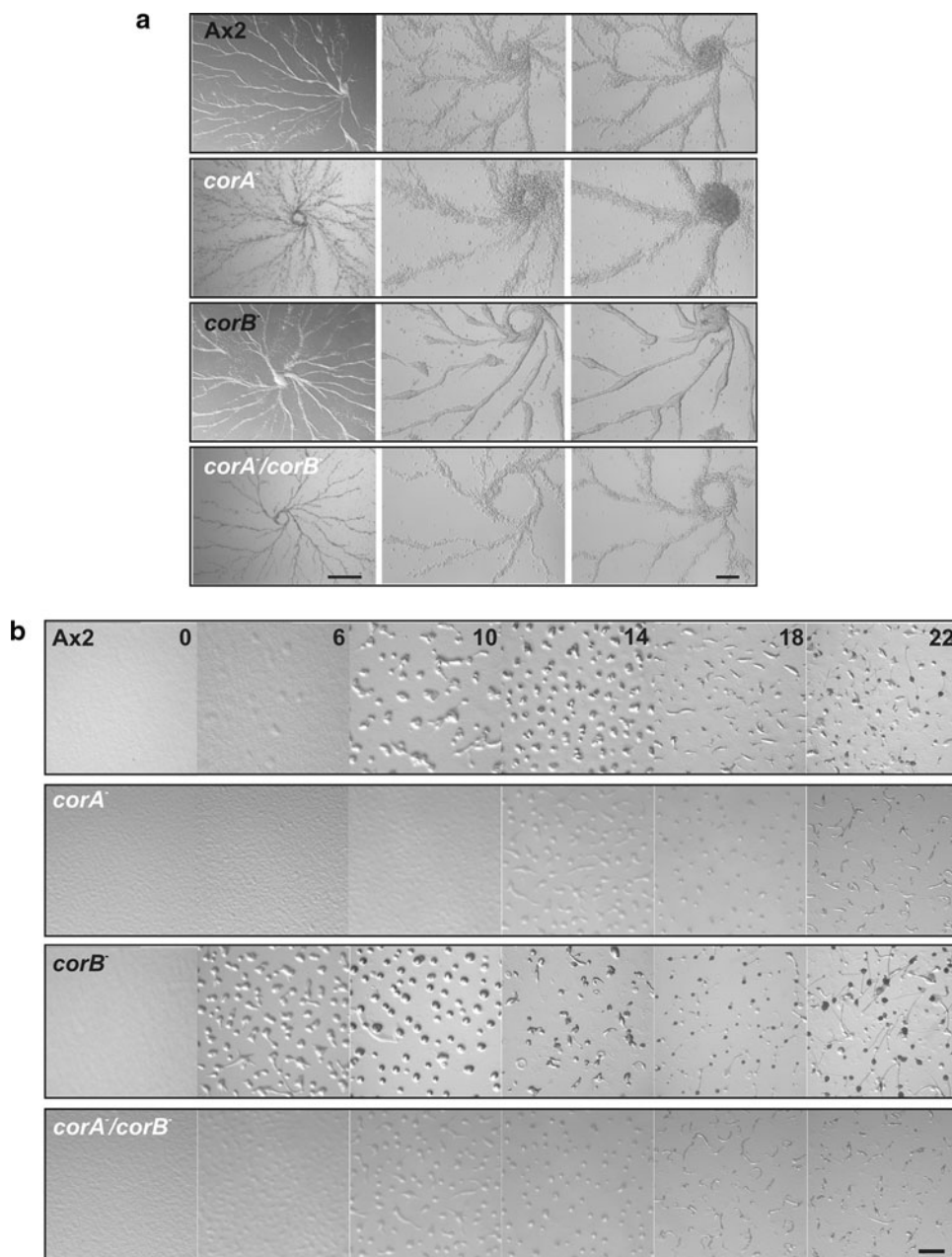


**Fig. 6** Coronin mutants show changes in developmental timing. **a** Stream formation under submerged conditions on a plastic surface.  $2 \times 10^5$  cells/cm<sup>2</sup> were starved under Sorensen phosphate buffer on plastic plates and monitored for aggregation. Representative images were taken at  $2.5\times$  (left) and  $10\times$  magnification (both panels at the right). Bar 1 cm and 200  $\mu\text{m}$ . **b** Development on non nutrient agar. For developmental analysis  $\sim 5 \times 10^7$  cells were deposited on a phosphate agar plate (10 cm in diameter). Development was recorded by video imaging over 24–30 h after onset of starvation. Representative pictures are shown. Bar 1 mm



bacteria and the *corA*<sup>-</sup>/*corB*<sup>-</sup>-double knockout strain behaved like the *corA*<sup>-</sup> strain showing uptake rates comparable to wild-type. The intracellular replication of the bacteria was not influenced by any of these mutations in our experiments (Fig. 8).

## Discussion

CRN12 and CRN7 are the only coronin proteins present in *D. discoideum*. They represent the two structural classes of coronins, the monomeric coronins and the coronin 7 type of coronins composed of two WD repeat domains. Monomeric

coronins can be classified into six vertebrate subfamilies, two nonvertebrate subfamilies and three further subfamilies, coronins 10, 11 and 12, at the base of the tree with members from alveolata, fungi and euglenozoa. The monomeric coronin of *D. discoideum*, CRN12, belongs to the most basic subfamily. Coronin 7 proteins show the broadest species distribution among protists, fungi, and metazoa, which suggests that they originated early in evolution by tandem duplication and fusion of a protozoan monomeric coronin [23].

CRN12 and CRN7 from *D. discoideum* have been described as cytoskeletal proteins with similar but not identical activities towards F-actin [9, 16, 22]. The



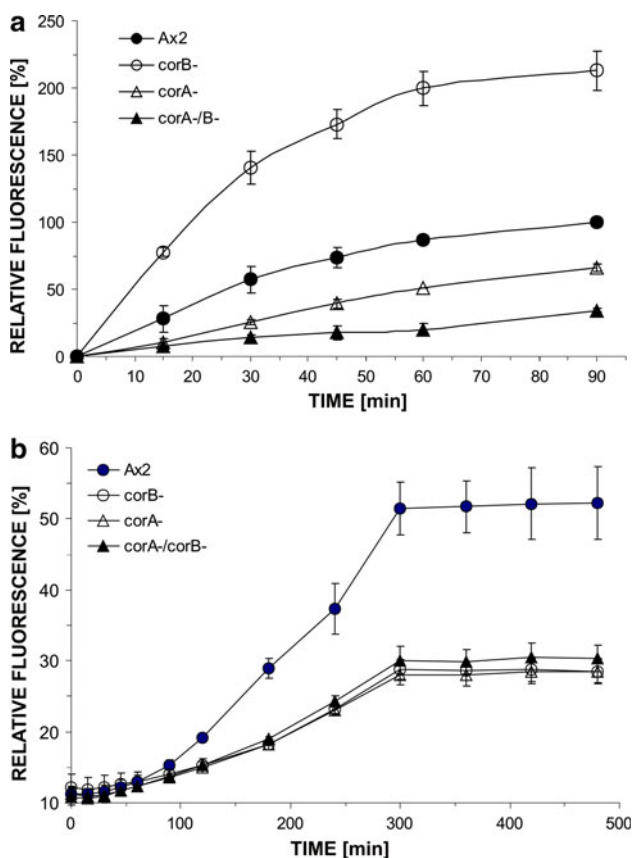


**Fig. 7** Phagocytosis of yeast and *E. coli* cells. **a** Quantitative analysis of TRITC-labeled yeast and **b** pHrodo *E. coli* uptake. Cells were resuspended at  $2 \times 10^6$  cells/ml in fresh axenic medium and an up to sixfold excess of fluorescent yeast cells and labeled bacteria as recommended by the supplier were added. Fluorescence of the internalized marker was measured at selected timepoints. In (a) data are presented as relative fluorescence that of Ax2 being considered as 100%. The data for Ax2 and *corB*<sup>-</sup> in (a) are from Shina et al. [16]

localization of both proteins overlaps to a large extent in immunofluorescence studies, furthermore they co-localize with F-actin stained by TRITC phalloidin.

In *D. discoideum*, a combination of chemotactic migration and differential cell adhesion is essential for all stages of its life cycle [39]. Morphogenesis starts with single amoebae which chemotactically aggregate when they starve, adhere to each other and form a multicellular organism undergoing morphogenetic changes. The main regulator of this process is cAMP which is secreted by the cells. cAMP acts in two ways. It alters gene transcription leading to the expression of development specific proteins and it induces changes in cell shape and chemotactic movement towards cAMP. Both events are essential for the ordered progression through the developmental life cycle that ends with the formation of a fruiting body. The actin cytoskeleton is one of the important targets of cAMP signaling as it controls cell shape formation and cell motility [33]. This proposition is supported by analysis of mutants

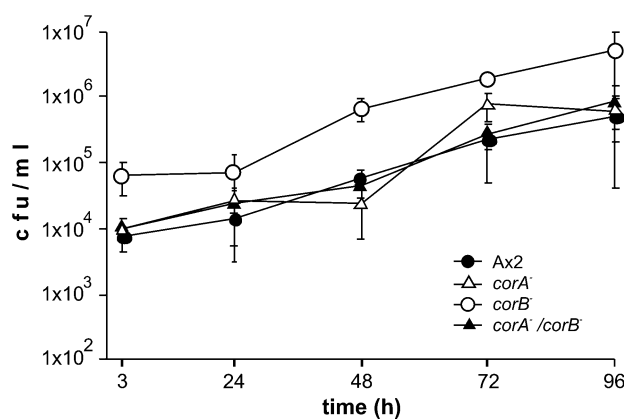


**Fig. 8** Infection of coronin mutants with *L. pneumophila*. Replication of *L. pneumophila* over 4 days was assessed in wild-type, *corA*<sup>-</sup>, *corB*<sup>-</sup> and *corA*<sup>-</sup>/*corB*<sup>-</sup> double knockout mutants. The graph represents the colony forming units (cfu) of the different time points post infection. With the exception of the *corB*<sup>-</sup> strain similar numbers of intracellular bacteria were detected 3 h post infection. Intracellular replication was monitored over 96 h by determining the cfu. The data for Ax2 and *corB*<sup>-</sup> are from Shina et al. [16]

in cytoskeletal proteins as well as in components that regulate the actin cytoskeleton. For example, myosin heavy chain deficient *D. discoideum* cells do not form fruiting bodies but stop already at the mound stage, an early stage of development. Mutants in which the activation of the small GTPase Rap which regulates actin assembly at the posterior pole during chemotaxis, is altered have a cell adhesion defect during aggregation and a cell patterning defect in the post aggregation stage [34, 40].

Disruption of the *corB* gene caused an accelerated development at early time points, whereas *corA*<sup>-</sup> mutants showed a delay in development of about 6 h. The developmental timing of the *corA*<sup>-</sup>/*corB*<sup>-</sup> mutant was comparable to wild-type Ax2 (Table 3). Furthermore, we observed significant impairment in motility and polarization in the *corA*<sup>-</sup> and *corA*<sup>-</sup>/*corB*<sup>-</sup> strains when we analyzed their behavior in a cAMP gradient. The *corB*<sup>-</sup> cells displayed no significant alterations in motility and polarization, although pseudopod extension initially occurred in a more random fashion (Table 2). Previously we had found that CRN7 associates with the Triton X-100 insoluble cytoskeleton after a cAMP stimulus. We concluded that CRN7 is not crucial for chemotactic behavior and the associated cytoskeletal reorganization but its presence makes these events more efficient. In case of the *corA*<sup>-</sup> and *corA*<sup>-</sup>/*corB*<sup>-</sup> mutants we observed a higher directional change and a rounder cell shape with respect to wild-type. When compared to the single *corA*<sup>-</sup> knockout cells the *corA*<sup>-</sup>/*corB*<sup>-</sup> cells showed a slight improvement with regard to polarity. Both parameters indicate a defect in proper polarization of the cells and therefore altered rearrangement and stability of the actin cytoskeleton under

**Table 3** Alterations found in coronin mutant cell lines

	<i>corB</i> <sup>-</sup>	<i>corA</i> <sup>-</sup>	<i>corA</i> <sup>-</sup> / <i>corB</i> <sup>-</sup>
Development	20 h	30 h	26 h
Motility/Chemotaxis	Not significantly impaired	Significantly impaired	Significantly impaired
Multinuclearity	Wild-type	Increased	Reduced as compared to <i>corA</i> <sup>-</sup>
Mitosis	Impaired	Impaired	Impaired
Phagocytosis of yeast	Increased	Decreased	Strongly decreased
Phagocytosis of <i>E. coli</i>	Decreased	Decreased	Decreased
Internalization of <i>L. pneumophila</i>	Increased	Wild-type	Reduced
Intracellular replication of <i>L. pneumophila</i>	Wild-type	Wild-type	Wild-type

Comparison and summary of phenotypes observed in *corA*<sup>-</sup>, *corB*<sup>-</sup> and *corA*<sup>-</sup>/*corB*<sup>-</sup> mutants in respect to the wild-type Ax2

conditions of the gradient. We suggest that although the cells can sense the cAMP gradient the signal cannot be translated into a correct cytoskeletal answer as might be also suspected from the F-actin response to a cAMP stimulus.

CRN12 and CRN7 localize to the phagocytic cup [10, 16] and *corA*<sup>-</sup> and *corB*<sup>-</sup> as well as the double knockout display changes in phagocytosis (Table 3). Phagocytosis is a combination of cellular adhesion, phagosome formation, uptake and phagosome maturation [37]. Whereas the *corA*<sup>-</sup> and the *corA*<sup>-</sup>/*corB*<sup>-</sup> show a decrease in the uptake of bacteria and yeast, *corB*<sup>-</sup> cells show a reduced uptake of *E. coli* but an increased uptake of yeast particles. For CRN12 a presence on vesicles of the endocytic pathway was reported where the protein associated with the endocytic compartment in an ordered fashion [41]. CRN7 was mainly present at the vesicles during uptake and lost from vesicles once they were internalized. The involvement in different processes may partially explain the observed defects.

Mechanisms that regulate phagocytosis play an important role in the host defence against invading microorganisms and several studies have addressed the relationship between coronins and the intracellular survival of pathogens [21, 37, 42]. In *D. discoideum* GFP-CRN12 was seen at the phagocytic cup upon internalization of *L. pneumophila* and was lost after 60 s. Furthermore, GFP-CRN12 was located in a heterogeneous fashion at *D. discoideum* compartments harboring bacteria [20]. In contrast to the GFP-CRN12 overexpressor and previous studies of the CRN12 knockout, *corA*<sup>-</sup> cells showed in our experiments no difference in uptake and replication of *L. pneumophila* with respect to wild-type.

The two coronin proteins in *D. discoideum* are both actin cytoskeleton associated proteins, they can bind to F-actin and they participate in the same cellular processes, in cytokinesis, phagocytosis, cell motility and chemotaxis, and in development. The comparison of the mutant phenotypes however shows no additive effects indicating that

the proteins act in independent pathways. In some of the processes studied, for example in development, they have opposing roles (Table 3). These findings support the proposal that CRN12 and CRN7 have different activities in the regulation of the actin dynamics with CRN12 promoting the disassembly of the filaments whereas CRN7 rather stabilizes filaments.

**Acknowledgments** This work was supported by grants from the DFG, by SFB 670 and by Köln Fortune.

## References

1. Appleton BA, Wu P, Wiesmann C (2006) The crystal structure of murine coronin-1: a regulator of actin cytoskeletal dynamics in lymphocytes. *Structure* 14:87–96
2. Goode BL, Wong JJ, Butty AC, Peter M, McCormack AL, Yates JR, Drubin DG, Barnes G (1999) Coronin promotes the rapid assembly and cross-linking of actin filaments and may link the actin and microtubule cytoskeletons in yeast. *J Cell Biol* 144:83–98
3. Cai L, Makhov AM, Schafer DA, Bear JE (2008) Coronin 1B antagonizes cortactin and remodels Arp2/3-containing actin branches in lamellipodia. *Cell* 134:828–842
4. Humphries CL, Balcer HI, D'Agostino JL, Winsor B, Drubin DG, Barnes G, Andrews BJ, Goode BL (2002) Direct regulation of Arp2/3 complex activity and function by the actin binding protein coronin. *J Cell Biol* 159:993–1004
5. Spoerl Z, Stumpf M, Noegel AA, Hasse A (2002) Oligomerization, F-actin interaction, and membrane association of the ubiquitous mammalian coronin 3 are mediated by its carboxyl terminus. *J Biol Chem* 277:48858–48867
6. Cai L, Makhov AM, Bear JE (2007) F-actin binding is essential for coronin 1B function in vivo. *J Cell Sci* 120:1779–1790
7. Galkin VE, Orlova A, Briehner W, Kueh HY, Mitchison TJ, Egelman EH (2008) Coronin-1A stabilizes F-actin by bridging adjacent actin protomers and stapling opposite strands of the actin filament. *J Mol Biol* 376:607–613
8. de Hostos EL, Bradtke B, Lottspeich F, Guggenheim R, Gerisch G (1991) Coronin, an actin binding protein of *Dictyostelium discoideum* localized to cell surface projections, has sequence similarities to G protein beta subunits. *EMBO J* 10:4097–4104
9. de Hostos EL, Rehfuess C, Bradtke B, Waddell DR, Albrecht R, Murphy J, Gerisch G (1993) *Dictyostelium* mutants lacking the

- cytoskeletal protein coronin are defective in cytokinesis and cell motility. *J Cell Biol* 120:163–173
10. Maniak M, Rauchenberger R, Albrecht R, Murphy J, Gerisch G (1995) Coronin involved in phagocytosis: dynamics of particle-induced relocalization visualized by a green fluorescent protein Tag. *Cell* 83:915–924
  11. Heil-Chapdelaine RA, Tran NK, Cooper JA (1998) The role of *Saccharomyces cerevisiae* coronin in the actin and microtubule cytoskeletons. *Curr Biol* 8:1281–1284
  12. Goode BL, Wong JJ, Butty AC, Peter M, McCormack AL, Yates JR, Drubin DG, Barnes G (1999) Coronin promotes the rapid assembly and cross-linking of actin filaments and may link the actin and microtubule cytoskeletons in yeast. *J Cell Biol* 144:83–98
  13. Sahasrabudhe AA, Nayak RC, Gupta CM (2009) Ancient *Leishmania* coronin (CRN12) is involved in microtubule remodeling during cytokinesis. *J Cell Sci* 122:1691–1699
  14. Jayachandran R, Sundaramurthy V, Combaluzier B, Mueller P, Korf H, Huygen K, Miyazaki T, Albrecht I, Massner J, Pieters J (2007) Survival of mycobacteria in macrophages is mediated by coronin 1-dependent activation of calcineurin. *Cell* 130:37–50
  15. Rybakin V, Clemen CS (2005) Coronin proteins as multifunctional regulators of the cytoskeleton and membrane trafficking. *Bioessays* 27:625–632
  16. Shina MC, Ünal C, Eichinger L, Müller-Taubenberger A, Schleicher M, Steinert M, Noegel AA (2010) A coronin7 homolog with functions in actin-driven processes. *J Biol Chem* 285:9249–9261
  17. Bharathi V, Pallavi SK, Bajpai R, Emerald BS, Shashidhara LS (2004) Genetic characterization of the *Drosophila* homologue of coronin. *J Cell Sci* 117:1911–1922
  18. Rybakin V, Stumpf M, Schulze A, Majoul IV, Noegel AA, Hasse A (2004) Coronin 7, the mammalian POD-1 homologue, localizes to the Golgi apparatus. *FEBS Lett* 573:161–167
  19. Rybakin V, Rastetter RH, Stumpf M, Uetrecht AC, Bear JE, Noegel AA, Clemen CS (2008) Molecular mechanism underlying the association of Coronin-7 with Golgi membranes. *Cell Mol Life Sci* 65:2419–2430
  20. Solomon JM, Leung GS, Isberg RR (2003) Intracellular replication of *Mycobacterium marinum* within *Dictyostelium discoideum*: efficient replication in the absence of host coronin. *Infect Immun* 71:3578–3586
  21. Solomon JM, Rupper A, Cardelli JA, Isberg RR (2000) Intracellular growth of *Legionella pneumophila* in *Dictyostelium discoideum*, a system for genetic analysis of host–pathogen interactions. *Infect Immun* 68:2939–2947
  22. Bretschneider T, Anderson K, Ecke M, Müller-Taubenberger A, Schroth-Diez B, Ishikawa-Ankerhold HC, Gerisch G (2009) The three-dimensional dynamics of actin waves, a model of cytoskeletal self-organization. *Biophys J* 96:2888–2900
  23. Morgan RO, Fernandez MP (2008) Molecular phylogeny and evolution of the coronin gene family. *Subcell Biochem* 48:41–55
  24. Claviez M, Pagh K, Maruta H, Baltes W, Fisher P, Gerisch G (1982) Electron microscopic mapping of monoclonal antibodies on the tail region of *Dictyostelium* myosin. *EMBO J* 1:1017–1022
  25. Peracino B, Wagner C, Balest A, Balbo A, Pergolizzi B, Noegel AA, Steinert M, Bozzaro S (2006) Function and mechanism of action of *Dictyostelium* Nramp1 (Slc11a1) in bacterial infection. *Traffic* 7:22–38
  26. Simpson PA, Spudich JA, Parham P (1984) Monoclonal antibodies prepared against *Dictyostelium* actin: characterization and interactions with actin. *J Cell Biol* 99:287–295
  27. Blau-Wasser R, Euteneuer U, Xiong H, Gassen B, Schleicher M, Noegel AA (2009) CP250, a novel acidic coiled coil protein of the *Dictyostelium* centrosome, affects growth, chemotaxis and the nuclear envelope. *Mol Biol Cell* 20:4348–4361
  28. Kilmartin JV, Wright B, Milstein C (1982) Rat monoclonal anti-tubulin antibodies derived by using a new nonsecreting rat cell line. *J Cell Biol* 93:576–582
  29. Schaap P (2007) Evolution of size and pattern in the social amoebas. *Bioessays* 29:635–644
  30. McArdle B, Hofmann A (2008) Coronin structure and implications. *Subcell Biochem* 48:56–71
  31. Neujahr R, Heizer C, Gerisch G (1997) Myosin II-independent processes in mitotic cells of *Dictyostelium discoideum*: redistribution of the nuclei, re-arrangement of the actin system and formation of the cleavage furrow. *J Cell Sci* 110:123–137
  32. Gaudet P, Williams JG, Fey P, Chisholm RL (2008) An anatomy ontology to represent biological knowledge in *Dictyostelium discoideum*. *BMC Genomics* 9:130
  33. Chisholm RL, Firtel RA (2004) Insights into morphogenesis from a simple developmental system. *Nat Rev Mol Biol* 7:531–541
  34. Elliott S, Joss GH, Spudich A, Williams KL (1993) Patterns in *Dictyostelium discoideum*: the role of myosin II in the transition from the unicellular to the multicellular phase. *J Cell Sci* 104:457–466
  35. McRobbie SJ, Newell PC (1983) Changes in actin associated with the cytoskeleton following chemotactic stimulation of *Dictyostelium discoideum*. *Biochem Biophys Res Commun* 115:351–359
  36. Fukui Y, Katsumaru H (1979) Nuclear actin bundles in Amoeba, *Dictyostelium* and human HeLa cells induced by dimethyl sulfoxide. *Exp Cell Res* 120:451–455
  37. Cosson P, Soldati T (2008) Eat, kill or die: when amoeba meets bacteria. *Curr Opin Microbiol* 11:271–276
  38. Maniak M (2002) Conserved features of endocytosis in *Dictyostelium*. *Int Rev Cytol* 221:257–287
  39. Dormann D, Weijer CJ (2006) Chemotactic cell movement during *Dictyostelium* development and gastrulation. *Curr Opin Genet Dev* 16:367–373
  40. Parkinson K, Bolourani P, Traynor D, Aldren NL, Kay RR, Weeks G, Thompson CR (2009) Regulation of Rap1 activity is required for differential adhesion, cell-type patterning and morphogenesis in *Dictyostelium*. *J Cell Sci* 122:335–344
  41. Rauchenberger R, Hacker U, Murphy J, Niewöhner J, Maniak M (1997) Coronin and vacuolin identify consecutive stages of a late, actin-coated endocytic compartment in *Dictyostelium*. *Curr Biol* 7:215–218
  42. Yan M, Collins RF, Grinstein S, Trimble WS (2005) Coronin-1 function is required for phagosome formation. *Mol Biol Cell* 16:3077–3087